Efficient Simulation of Rarefied Gas Flows Through Tubes of Finite Length Based on Kinetic Model Equations

S.Pantazis and D.Valougeorgis

Department of Mechanical Engineering, University of Thessaly, Pedion Areos, 38334 Volos, Greece

Abstract. The flow of a rarefied gas through tubes of circular cross-section and finite length, driven by arbitrarily large gradients of pressure is simulated in a computationally efficient manner based on kinetic model equations. The governing Ellipsoidal model kinetic equation is discretized in the phase space by a finite difference scheme and the discrete velocity method. It is seen that good agreement is obtained with corresponding DSMC results in the literature. Due to the five-dimensional nature of the problem, various techniques have been used to reduce the computational effort. Convergence has been accelerated for small Knudsen flows using the Wynn-epsilon algorithm while memory usage optimization, grid refinement and parallelization have been introduced. Overall, a highly efficient deterministic algorithm has been developed.

Keywords: Non-linear kinetic equations, finite length
PACS: 47.45.Ab, 47.45.-n

INTRODUCTION

The simulation of rarefied flows is a challenging task with significant practical applications in several fields, such as in vacuum [1, 2] and Micro Electronic Mechanical Systems (MEMS) [3, 4] industry. In practice, the gas may be close or far from equilibrium in different positions of the same apparatus and approaches capable of dealing with multiple levels of rarefaction are often required. The kinetic theory of gases is usually employed to deal with such problems in a unified manner. As the complexity increases for high-dimensional problems, the Direct Simulation Monte Carlo (DSMC) method [5] is usually preferred over the use of kinetic equations. However, this method is associated with large computational effort, certain difficulties in the parallelization of the code and statistical noise for low speed flows, while in the solution of high speed flows its performance is excellent. On the other hand, deterministic methods are more appropriate for low Mach numbers, where the transport equations are simplified due to linearization and their solution is obtained very efficiently due to the proposed acceleration schemes [6].

However, by implementing the non-linear form of collisional models, flows induced by arbitrarily large pressure differences can also be studied as an alternative to DSMC. This type of treatment is applied here for the solution of flow through a tube of finite length, driven by large gradients of pressure. An enhanced algorithm is proposed by applying certain computational techniques. In particular, the total number of iterations is significantly reduced by the Wynn-epsilon acceleration [7, 8], the code is parallelized and memory demands are reduced by proper handling of the allocated arrays. The efficiency of the algorithm is described and a preliminary comparison with recently obtained DSMC results [9] is provided. Our objective is to provide a fully deterministic algorithm for solving non-linear kinetic equations and obtain results with computational efficiency similar to that of the DSMC method.

FORMULATION

Consider a monatomic rarefied gas stored in two large reservoirs connected by a cylindrical tube of radius R and length L. An arbitrarily large pressure difference is imposed between the two containers, causing flow of the gas through the tube. The two containers and the wall of the tube are maintained at the same temperature T_0.

The geometry, consisting of the circular tube and efficiently large parts of the reservoirs, is displayed in Fig. 1. The coordinate system in the physical space $(\hat{r},\hat{z})$ and the molecular velocity coordinate system $(\xi_r,\xi_\vartheta,\xi_z)$ are also shown in the same figure. The symbol ϑ denotes the direction normal to the $\hat{r}-\hat{z}$ plane, while θ is the molecular velocity angle in the $\hat{r}-\vartheta$ plane. A cylindrical coordinate system (ξ_p,θ,ξ_z) using $\xi_r=\xi_p\cos\theta$ and $\xi_\vartheta=\xi_p\sin\theta$ is preferred here.

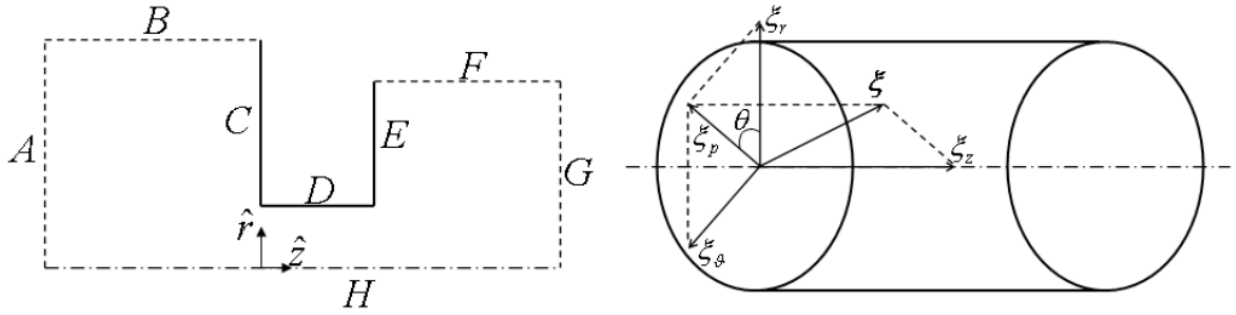

Figure 1. Flow configuration and coordinate system

The starting point is the ellipsoidal (ES) model kinetic equation [10] in cylindrical coordinates, expressed as

$$\xi_r \frac{\partial f}{\partial \hat{r}} - \frac{\xi_\vartheta}{\hat{r}} \frac{\partial f}{\partial \theta} + \xi_z \frac{\partial f}{\partial \hat{z}} = \nu \left(f^{ES} - f \right) \tag{1}$$

with $f = f(\hat{r}, \hat{z}, \xi_r, \xi_\vartheta, \xi_z)$ being the distribution function and $\xi_i, i = r, \vartheta, z$ the components of the molecular velocity. The collision term is retained in its non-linear form with

$$f^{ES} = \frac{n}{\pi^{3/2}} \sqrt{|A|} \exp \left[- \sum_{i,j=1}^{3} (\xi_i - \hat{u}_i) A_{ij} (\xi_j - \hat{u}_j) \right] \tag{2}$$

where $A = \left[(2 k_B T \delta_{ij}) / (m \mathrm{Pr}) - 2 (1 - \mathrm{Pr}) \hat{P}_{ij} / (nm \mathrm{Pr}) \right]^{-1}$, Pr is the Prandtl number, k_B is the Boltzmann constant, m is the molecular mass and δ_{ij} the Kronecker delta. Here, n, T, $\hat{u}_i$ are the number density, temperature and gas bulk velocity components, respectively. By substituting $\mathrm{Pr} = 1$ it can be seen that the BGK expression is retrieved. The characteristic value for monatomic gases, $Pr = 2/3$, has been used in the following calculations.

The number density, pressure and temperature of the left reservoir are chosen as reference quantities and they are denoted by n_0, T_0, P_0 with $P_0 = n_0 k_B T_0$. Then, all quantities of interest are non-dimensionalized as follows:

$$r = \frac{\hat{r}}{R}, \quad z = \frac{\hat{z}}{R}, \quad c_i = \frac{\xi_i}{\upsilon_0}, \quad g = \frac{f \upsilon_0^3}{n_0}, \quad \rho = \frac{n}{n_0}, \quad u_i = \frac{\hat{u}_i}{\upsilon_0}, \quad \tau = \frac{T}{T_0}, \quad P = \frac{\hat{P}}{P_0}, \quad P_{ij} = \frac{\hat{P}_{ij}}{P_0}, \quad i, j = r, \vartheta, z \tag{3}$$

with $\upsilon_0 = \sqrt{2 k_B T_0 / m}$ being the most probable molecular velocity and $\hat{P}_{ij}$ being the stress tensor.

The collision frequency is given for Hard Sphere interaction by the expression

$$\nu = \frac{P}{\mu} Pr = \delta_0 \rho \sqrt{\tau} \frac{\upsilon_0}{R} Pr \tag{4}$$

where μ is the dynamic viscosity. The rarefaction parameter of the flow δ_0 is also defined here as

$$\delta_0 = \frac{R P_0}{\mu_0 \upsilon_0} = \frac{\sqrt{\pi}}{2} \frac{1}{Kn_0} \tag{5}$$

with μ_0 being the gas viscocity at reference temperature T_0. The rarefaction parameter is proportional to the inverse of the Knudsen number and therefore as δ_0 is increased the atmosphere becomes more dense (or less rarefied). The cases of $\delta_0 = 0$ and $\delta_0 \to \infty$ correspond to the free molecular and hydrodynamic limits respectively.

The final form of the governing equation is

$$c_p \cos\theta \frac{\partial g}{\partial r} - \frac{c_p \sin\theta}{r} \frac{\partial g}{\partial \theta} + c_z \frac{\partial g}{\partial z} = \delta_0 \rho \sqrt{\tau} Pr \left(g^{ES} - g \right) \tag{6}$$

where the dimensionless ES model term is

$$g^{ES} = \frac{\rho}{\pi^{3/2}} \mathrm{Pr}^{3/2} \sqrt{|K|} \exp \left[- \mathrm{Pr} \sum_{i,j=1}^{3} (c_i - u_i) K_{ij} (c_j - u_j) \right] \tag{7}$$

with $K=[\tau\delta_{ij}-(1-\mathrm{Pr})P_{ij}/\rho]^{-1}$.

It is seen that the well known projection procedure can not be implemented here because all molecular velocity components are required. Thus, in the following we have $c^2=c_p^2+c_z^2$. Furthermore, we only examine velocity angles in $\theta\in[0,\pi]$ and assume the distribution is axisymmetrical.

The macroscopic quantities are also non-dimensionalized, leading to the following expressions:

$$\rho=2\int_0^\infty\int_0^\pi\int_{-\infty}^\infty c_p g dc_z d\theta dc_p,\quad \tau=\frac{4}{3\rho}\int_0^\infty\int_0^\pi\int_{-\infty}^\infty c_p\left[(c_p\cos\theta-u_r)^2+(c_p\sin\theta)^2+(c_z-u_z)^2\right]g dc_z d\theta dc_p \tag{8}$$

$$u_r=\frac{2}{\rho}\int_0^\infty\int_0^\pi\int_{-\infty}^\infty c_p^2\cos\theta g dc_z d\theta dc_p,\ u_z=\frac{2}{\rho}\int_0^\infty\int_0^\pi\int_{-\infty}^\infty c_p c_z g dc_z d\theta dc_p,\ P_{ij}=2\int_0^\infty\int_0^\pi\int_{-\infty}^\infty c_p\left(c_i-u_i\right)\left(c_j-u_j\right)g dc_z d\theta dc_p$$

Vector/tensor components containing the ϑ-direction once, i.e. $u_\vartheta, p_{r\vartheta}, p_{z\vartheta}, q_\vartheta$, are zero, while $p_{\vartheta\vartheta}$ is not. Pressure can be easily derived by $P=\rho\tau$.

The inlet and outlet boundary distributions are Maxwellians. Due to the reference values selection, we have $P_0=1$ for the left, $\Pi=P_1/P_0$ for the right container boundary distributions and $\tau=1$ at all boundary surfaces. Therefore, all incoming molecules conform to a Maxwellian

$$g^+=\frac{C}{\pi^{3/2}}\exp\left(-c^2\right) \tag{9}$$

where $C=1$ on the left container, $C=\Pi$ on the right and $C=\rho_w$ on the walls. The ρ_w constants are found by imposing the impermeability condition at each wall

$$\rho_{w,i}=4\sqrt{\pi}sA_i, i=C,D,E \tag{10}$$

$$A_C=\int_0^\infty\int_0^\pi\int_0^\infty c_z c_p g^- dc_z d\theta dc_p\quad A_D=\int_0^\infty\int_0^{\pi/2}\int_{-\infty}^\infty c_p^2\cos\theta g^- dc_z d\theta dc_p\quad A_E=\int_0^\infty\int_0^\pi\int_{-\infty}^0 c_z c_p g^- dc_z d\theta dc_p \tag{11}$$

where $s=1$ for walls C,D and $s=-1$ for wall E. Specular reflection is imposed at the center due to the axial symmetry.

$$g^+\left(0,z,c_p,\theta,c_z\right)=g^-\left(0,z,c_p,\pi-\theta,c_z\right)$$

for angles in $\theta\in[0,\pi/2]$.

THE NUMERICAL METHOD AND ITS OPTIMIZATION

The discrete velocity method is applied for the treatment of the molecular velocity space. The continuum spectrum of c_p and c_z are discretized by the Legendre polynomial roots mapped in $[0,c_{p,max}]$ and $[0,c_{z,max}]$ respectively, while the molecular velocity angles are uniformly distributed in $[0,\pi]$ due to the axisymmetry.

The solution algorithm is an iterative procedure leading to the determination of the distribution function. At first, an assumption is made for the macroscopic quantity profiles. This estimation is used in combination with the governing equation to calculate the value of the distribution function. The distribution function is further used to generate new values for the bulk quantities via the corresponding moments. Finally, these quantities are provided as feedback to the governing equation to obtain new estimates and this procedure is repeated until a proper convergence criterion, imposed on the bulk quantities, is satisfied.

The second order diamond difference scheme has been applied here, derived by integrating the governing equation (6) in r,θ,z in an arbitrary discretization interval, in the same way as in [7]. Due to the $1/r$ terms, this expression is usable at $r=0$ only after the application of the "De l'Hospital" rule.

The accuracy and convergence of the numerical method have been improved by the use of the Wynn-epsilon algorithm [7, 8]. The Wynn-epsilon algorithm is a strongly nonlinear sequence accelerator, applied in regular iteration intervals on the macroscopic quantities and the impermeability constants to obtain a converged solution faster. The convergence of a sequence S_j, $j=1,...,J$, can be accelerated by forming a tableau whose even columns are estimations of the sequence limit

$$\varepsilon_{l+1}^{(j)}=\varepsilon_{l-1}^{(j+1)}+\left[\varepsilon_l^{(j+1)}-\varepsilon_l^{(j)}\right]^{-1} \tag{12}$$

with $\varepsilon_{-1}^{(j)} = 0$ and $\varepsilon_0^{(j)} = S_j$. It is important to numerically monitor the values of each sequence and ensure that the sequence is converging. The outcome of this examination is required in order to decide whether it is best to apply the acceleration algorithm or not.

The application of the above technique can reduce the computational time by at least an order of magnitude near the hydrodynamic regime. Furthermore, "false convergence" effects, appearing in large δ, are significantly reduced. Finally, another important feature of this method is that it can also be easily applied with linearized kinetic equations after some minor modifications.

Further computational optimizations can be obtained by noticing that the distribution functions of different velocity magnitudes can be calculated independently from one another. This fact leads to a straightforward parallelization of the code. Each processor solves the kinetic equation for a group of velocities and information on macroscopic quantities and impermeability constants is exchanged between the processors at the end of each iteration. In this manner, the transmition of the distribution is circumvented, greatly reducing the cost of parallel communication.

Memory handling techniques had also to be used to reduce storage requirements due to the five-dimensional nature of the distribution function for this problem. Due to the velocity magnitude independency, a temporary array can be allocated and overwritten after treating each magnitude. Furthermore, the dimensionality of this array can be reduced even more by storing the distribution only in the parts of the domain required by the marching scheme of the discretized governing equation. For example, for motion towards the positive z direction, the distribution is stored only at positions z and $z - \Delta z$. These techniques permit having a two-dimensional array for the distribution function and practically remove memory limitations. In this manner, tubes of any length can be considered, since the size of this array is only determined by the height of the entrance/exit regions and the number of the molecular velocity angles.

The discretization parameters used are displayed in Table 1. It is noted that the initial grid contains 20 intervals per unit length in every direction and 20 angle intervals in [0, Pi]. The simulations are initially performed with a smaller amount of nodes and angles. After convergence has been reached, the simulation procedure is repeated in a refined mesh, where the grid parameters have been doubled, using the previous solution as an initial condition. This procedure is repeated until the final number of nodes and angles has been reached in order to avoid a large number of iterations for the dense grid, leading to great savings for large values of δ. For the results shown here, the total number of physical nodes in the final grid level may be up to 3.3×10^6. The average residual per computational node has been chosen as the convergence criterion.

Table 1. Computational parameters

Final nodes per unit length	160
Final discrete angles in $(0, \pi)$	160
Discrete magnitudes c_p and c_z	16×16
Maximum value of velocity magnitude c_{max}	5
Convergence criterion	2.5×10^{-7}

RESULTS

The main quantity of interest for the current problem is the mass flow rate through the tube, denoted by $\dot{M}$. Its dimensionless form is

$$W = \frac{\dot{M}}{\dot{M}_0} = 4\sqrt{\pi} \int_0^1 \rho u_z r dr \tag{13}$$

where the corresponding free molecular analytical result for flow through an orifice into vacuum $\dot{M}_0 = \sqrt{P_0} \pi R^2 / \upsilon_0$ is taken as a reference quantity. Results are presented here for the case $L = R$.

Comparison with DSMC results has shown very good agreement for both flow rates and macroscopic quantity distributions. It is seen that the flow rates, presented in Table 2 for $\Pi = 0.1$ and 0.5, are within 2% agreement near the free molecular and hydrodynamic regime and 6% in the transition regime with those found in [9]. It must be noted that our purpose here is not to make a direct comparison with DSMC. Due to the existence of many DSMC algorithms and the stochastic nature of the method, it is difficult to ensure that the comparison will take place on the same basis.

The required computational effort in hours and the gain in speed due to the parallelization are displayed in Fig. 2, using a number of CPUs varying from 16 to 256. At all cases, the simulations are finished within a few tens of hours at most, even with a low number of processors. The scaling characteristics of the algorithm are quite good,

considering the number of variables that have to be exchanged at each iteration. The speed-up $S(n)$, defined as $S(n) = [t(8) \times 8] / [t(n) \times n]$ with n being the number of CPUs and $t(n)$ the simulation time, is also displayed here. An average efficiency of about 94% for 64 processors and 75% for 256 processors is calculated. It is expected that parallelizing in the spatial coordinates as well would greatly reduce the cost of exchanging information, since only a part of the domain would be stored at each computational node. Finally, it is noted that Wynn-epsilon acceleration has not been applied while timing the simulations in order to obtain a more accurate picture of the performance of the code.

The benefits of starting with a sparse grid and gradually refining it are seen in Table 3. The solution of each grid level is used as an initial condition for the simulation of the next level. Linear interpolation has been used here as a first approximation. It is clear that the gain in the number of iterations for large values of δ is significant. The iterations in dense grids are two orders of magnitude lower than the corresponding sparse grid number, leading to much lower simulation times.

The effect of Wynn-epsilon acceleration is demonstrated through an indicative case ($\delta = 10, \Pi = 0.1$) shown in Fig. 3. The evolution of the residual is plotted against the number of iterations for both a normal and an accelerated run. Both cases follow the same course for the first 500 iterations, to allow for a transitional stage before applying the acceleration scheme. Then, the sequence terms are collected every two iterations until 81 terms have been collected. Finally, Equation (12) is applied at iteration 660 as shown in Fig. 3, causing an abrupt spike in the residual of the accelerated run. However, after this step, the residual of the accelerated run drops dramatically, leading to convergence in less than half the iterations required for a normal run. The algorithm proves to be quite useful near the hydrodynamic regime, where a reduction in the number of iterations up to 75% has been observed in other problems for $\delta = 650$ [7].

To sum up, an efficient algorithm for the solution of non-linear kinetic equations has been presented and applied to the pressure driven isothermal flow through a circular tube. The flow rates and macroscopic quantities are in good agreement with previously reported results obtained by the DSMC method. The computational effort and memory demands are drastically reduced by the implementation of Wynn-epsilon acceleration, as well as memory usage optimization, grid refinement and parallelization.

Table 2. Dimensionless flow rate G for isothermal pressure driven flow through a tube with $L/R = 1$

	δ	0.0	0.1	0.5	1.0	2.0	5.0	10.0	20.0
$\Pi = 0.1$	ES	0.605	0.619	0.665	0.712	0.786	0.930	1.05	1.16
	DSMC	0.605	0.613	0.648	0.689	0.761	0.913	1.05	1.16
$\Pi = 0.5$	ES	0.336	0.347	0.384	0.427	0.503	0.689	0.883	1.04
	DSMC	0.336	0.343	0.370	0.405	0.474	0.658	0.866	1.04

Table 3. Effect of grid refinement on the number of iterations

Grid level	Nodes per unit length	Velocity angles	Iterations for $\delta = 0.1$	Iterations for $\delta = 1$	Iterations for $\delta = 10$	Iterations for $\delta = 20$
1	20	20	12	77	1800	4746
2	40	40	5	12	72	149
3	80	80	5	9	49	83
4	160	160	4	7	37	63

ACKNOWLEDGMENTS

The authors gratefully acknowledge support by the Association Euratom - Hellenic Republic. The views and opinions expressed herein do not necessarily reflect those of the European Commission. The authors are also grateful to Prof. Barry Ganapol of the University of Arizona for helpful discussions and supportive material on the implementation of the acceleration schemes.

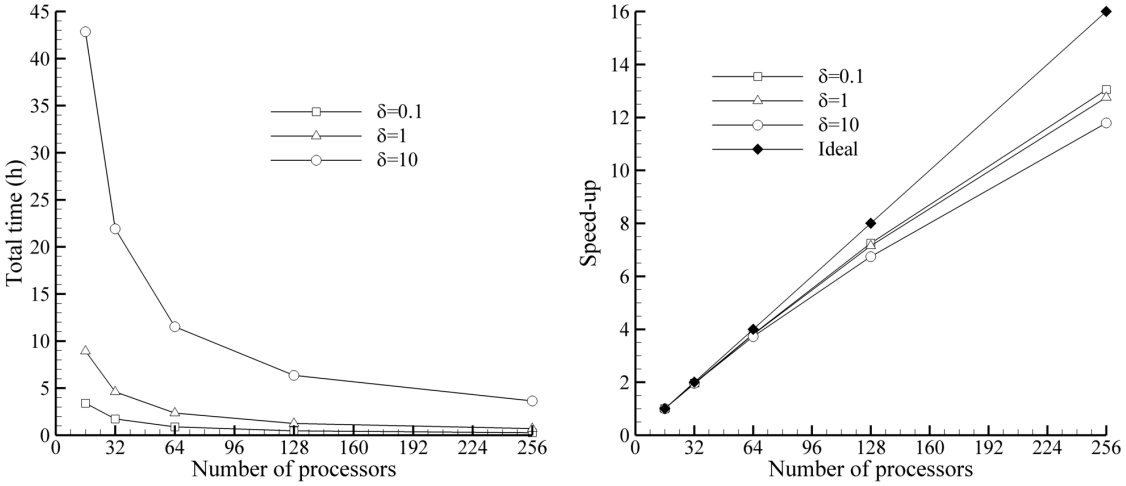

Figure 2. Total time (left) and speed up (right) for various δ and $\Pi = 0.1$

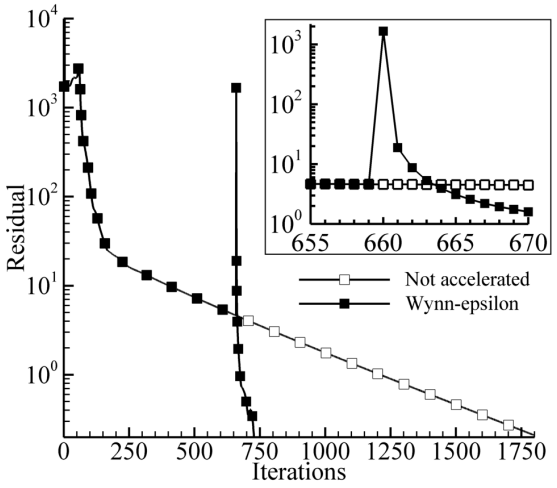

Figure 3. Wynn-epsilon effect on the residual for $\delta = 10$,$\Pi = 0.1$

REFERENCES

1. C. Day, D. Murdoch, *Journal of Physics: Conference Series* **114** (2008).
2. F. Sharipov, P. Fahrenbach, A. Zippa, *J. Vac. Sci. Technol. A* **23(5)** (2005).
3. C.M. Ho, Y.C. Tai, *Annu. Rev. Fluid Mech.* **30**, 579–612 (1998).
4. J.M. Reese, M.A. Gallis, D.A. Lockerby, *Phil. Trans. R. Soc. Lond. A* **361**, 2967–2988 (2003).
5. G. A. Bird, *Molecular Gas Dynamics and the Direct Simulation of Gas Flows*, Oxford University Press, Oxford, 1994.
6. D. Valougeorgis, S. Naris, *SIAM Journal of Scientific Computing* **25 (2)**, 534–552 (2003).
7. S. Pantazis, D. Valougeorgis, *European Journal of Mechanics B/Fluids* (2010), doi:10.1016/j.euromechflu.2010.05.004.
8. B. D. Ganapol, *Z. angew. Math. Phys.* **57**, 1011–1024 (2006).
9. S. Varoutis, D. Valougeorgis, F. Sharipov, *J. Vac. Sci. Technol. A* **27 (6)** (2009).
10. L.H. Holway, *Physics of fluids* **9** (1966).